Overview of Transport, Fast Particle and Heating and Current Drive Physics using Tritium in JET plasmas

D.Stork 1), Yu. Baranov 1), P.Belo 2), L.Bertalot 3), D.Borba 2), J.H.Brzozowski 4), C.D.Challis 1), D.Ciric 1), S. Conroy 5), M.de Baar 6), P.de Vries 1), P Dumortier 7), L.Garzotti 8), N.C.Hawkes 1), T.C.Hender 1), E.Joffrin 9), T.T.C.Jones 1), V.Kiptily 1), P.Lamalle 7), J.Mailloux 1), M.Mantsinen 10), D.C.McDonald 1), M.F.F.Nave 2), R.Neu 11), M. O'Mullane 1), J.Ongena 7), R.J.Pearce 1), S.Popovichev 1), S.E.Sharapov 1), M.Stamp 1), J.Stober 11), E.Surrey 1), M.Valovic 1), I.Voitsekhovitch 1), H.Weisen 12), A.D.Whiteford 13), L.Worth 1), V.Yavorskij 14), K-D.Zastrow 1) and JET EFDA contributors †.

1) Euratom/UKAEA Fusion Association, Culham Science Centre, Abingdon, UK.
2) Euratom/IST Fusion Association, Lisboa, Portugal
3) Associazione EURATOM-ENEA sulla Fusione, Frascati, Italy
4) Alfven Laboratory, EURATOM-VR Asociation, Stockholm, Sweden
5) Dept. of Neutron Res., Uppsala University, EURATOM-VR Association, Uppsala, Sweden
6) FOM Instituut voor Plasmaphysica, Associate Euratom, Nieuwegein, The Netherlands
7) LPP-ERM/KMS, EURATOM-Belgian State Association, Brussels, Belgium
8) Consorzio-RFX, Associazione EURATOM-ENEA sulla Fusione, Padova, Italy
9) Association EURATOM-CEA sur la Fusion, CEA Cadarache, St Paul-lez-Durance, France.
10) Helsinki Univ. of Technology, Association EURATOM-TEKES, Finland.
11) Max-Planck Institut fur Plasmaphysik, EURATOM Assoziation, Garching, Germany
12) CRPP, Association EURATOM-Confédération Suisse, Lausanne, Switzerland
13) Dept. of Physics, University of Strathclyde, Glasgow, UK
14) Inst. for Theoretical Physics, Univ. of Innsbruck, Association EURATOM-OEAW, Austria.

email contact of main author: derek.stork@jet.efda.org

Abstract. Results are presented from the JET Trace Tritium Experimental (TTE) campaign using minority tritium (T) plasmas (n_T/n_D<3%). Thermal tritium particle transport coefficients (D_T, v_T) were found to exceed neo-classical values in all regimes except in ELMy H-modes at high density , and in the region of Internal Transport Barriers (ITB) in Reversed shear plasmas. In hybrid scenarios (q_{min}~1, low positive shear, no sawteeth), T particle confinement was found to scale with increasing triangularity and plasma current. In ELMy H-mode dimensionless parameter scans, T particle transport scaled in a Gyro-Bohm manner in the inner plasma (r/a<0.4), whilst the outer plasma particle transport behaved more like Bohm scaling. Dimensionless parameter scans showed contrasting behaviour for particle confinement (increases with collisionality ν* and β) and energy confinement (decreases with ν^* and independent of β). Comparing regimes (ELMy H-mode, ITB plasma, and Hybrid scenarios) outside the central plasma region (0.65<r/a<0.85), normalised tritium diffusion (D_T/B_ϕ) scaled with normalised poloidal Larmor radius ($\rho_\theta^*=q\rho^*$) in a manner close to Gyro-Bohm (~ρ_θ^{*3}), with an added inverse β dependence. The effects of ELMs, sawteeth and Neo-classical tearing modes (NTMs) on T particle transport are described. Fast-ion confinement in Current-Hole (CH) plasmas, was tested in TTE by injection of Tritium NBI into JET CH plasmas. γ-rays from the reactions of fusion alphas and beryllium impurities (^{9}Be(α,nγ)^{12}C) characterised the fast fusion-alpha population evolution. The γ-decay times were consistent with classical alpha plus parent fast triton slowing down times ($\tau_{Ts}+\tau_{\alpha s}$) for high plasma currents (I_p >2MA) and monotonic q-profiles. In CH discharges the γ-ray emission decay times were much lower than classical ($\tau_{Ts}+\tau_{\alpha s}$), indicating alpha confinement degradation, due to orbit losses predicted by a 3-D Fokker Planck numerical code, and modelled by TRANSP.

---

† See Annex of J Pamela et al., this conference, Paper OV/1-2

1. Introduction

The JET Tokamak is the only magnetic confinement fusion device which has the capability of operating with deuterium-tritium (D-T) plasmas, including Tritium Neutral Beam Injection (NBI). D-T plasmas with concentration ratios in the range 10:90 < T:D < 90:10 have been exploited in previous campaigns studying fusion plasma phenomena [1]: including the generation of fusion power up to 16 MW; the demonstration of alpha-particle heating in high performance regimes; and in scaling of the ELMy H-mode behaviour of D-T plasmas towards ITER. Tritium is also useful in the study of particle transport. The evolution of the tritium spatial distribution can be detected in "trace" (typically $n_T/(n_D+n_T)<3\%$ are used in experiments) quantities by observation of the 14 MeV neutron emission, allowing non-perturbative transient experiments using a fuel ion species. Thus, "trace tritium" experiments allow convection (v_T) and diffusion (D_T) to be measured separately, unlike particle transport studies on deuterium ions in steady-state plasmas. In the latter only the ratio v_D/D_D, can be measured, and there are significant problems of source identification and ion density measurement. Previous 'trace tritium' experiments have been conducted on JET in 1997 [2, 3] and on TFTR [4, 5].

The JET Trace Tritium Experimental (TTE) campaign, reported in this paper, took place in September –October 2003, and whilst the core of the campaign focussed on particle transport, many other physics issues were addressed. The campaign featured experiments on: thermal particle (fuel ion) transport in a number of regimes and scenarios; fast ion transport and confinement; effects of MHD phenomena on thermal and fast-ion transport; and Ion Cyclotron Resonance Heating (ICRH) of tritium minority species. This paper gives an overview of results in these fields and indicates work still in progress. The campaign also produced significant results in development of 14 MeV neutron diagnostics. These are reported in a companion paper [6].

2. General Experimental Conditions

Technical details of the systems involved in the TTE Campaign are given in [7]. Tritium was introduced into JET by short, 80 ms, T_2 gas puffs of ≤ 6 mg, or by short (typically 200 ms) pulses with T^0-NBI (~100 keV, 1 MW). The time evolution of the tritium gas source entering the plasma was accurately measured locally with 10 ms time resolution from Tα emission on a line-of-sight local to the inlet valve. The detailed shape of the gas flow could be measured in L-mode discharges and was established as invariant in all discharges where it was measured, giving an accurate time-stamp for the start of the tritium transport analysis. Following the gas puff, about 10% of the tritium puffed was found inside the plasma by the time of peak neutron emission (in contrast to T^0-NBI which has near 100% fuelling efficiency). The rest of the tritium gas after the puff was in the vessel wall and divertor tiles. Tritium released from these components acted as a source and could affect the transport results (see below). To minimise the effect, frequent 'clean-up' pulses were run in pure D-D plasmas, keeping the tritium wall inventory to a minimum.

The neutron emission from DD and DT reactions was measured spatially with a nineteen-channel neutron profile monitor and by Silicon-diode detectors for the total neutron rate [8, 9]. The profile monitor has ten horizontal and nine vertical lines-of-sight; these are overlayed on the emissivity contours shown in Fig. 1. All channels are absolutely calibrated at 2.5 MeV for DD and 14 MeV for DT reactions, and provide 10 ms time resolution.

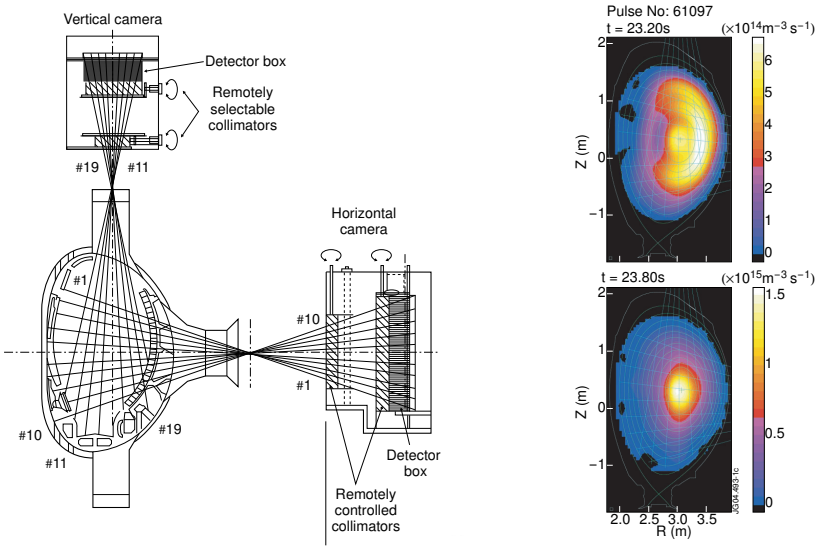

Fig.1 (Left) Schematic overview of the JET neutron camera, showing lines of sight.(Right) Comparison of 14 MeV emissivity contours for a shot with tritium gas puff. Top figure shows contours 150 ms after the puff, when the tritium density is hollow. Bottom figure shows peaked shape after 750 ms once the tritium density profile has relaxed. Initial crescent shape is due to the poloidal distribution of fast NBI deuterium ions.

The outermost channels of the camera with good statistics are channels #9(horizontal) and #19(vertical), with typically r/a=0.82. Thus valid particle transport results were obtained in the TTE Campaign for the plasma inside r/a≈0.85.

3. Thermal particle transport analysis and results

The TTE Campaign produced data that will enable investigation of several aspects of thermal particle transport: fuel-ion particle transport dimensionless-parameter scaling in ELMy H-modes; fuel-ion particle transport in various ELMy H-modes scenarios – high vs low density, plasmas with high ICRF heating, impurity-seeded discharges; effects of sawteeth and ELMs on fuel-ion transport; fuel-ion transport in Internal Transport Barrier (ITB) and hybrid scenarios;confinement effects on thermal ions of neo-classical tearing modes (NTMs).

Data from selected channels of the 14 MeV neutron profile monitor are shown in Fig 2(a). Following the tritium puff, the 14 MeV signal rose on all channels as the tritium ions diffuse inward. During this rise phase, the data are used to derive values for D_T and v_T. In the following phase, once the tritium ion profiles were centrally peaked, the gradients drove the ions from the plasma, and during this relaxation, only the ratio v_T/D_T can be determined as a cross-check. As the tritium gas puff did not perturb plasma parameters, the transport coefficients are assumed to be constant in time for ELMy H-Mode and hybrid scenario discharges, whereas radial movement of transport barriers is allowed for ITB discharges. The details of the least-squares fitting of data from the neutron profile monitor and neutron yield with a transport model for tritium with free parameters for the spatial profiles of D_T and v_T and the influx are given in reference [10].

The fits to the data show that tritium transport exceeds neo-classical levels in most ELMy H-mode cases studied, only approaching neo-classical levels in ELMy H-modes at high density in low current, low q_{95} discharges (see Fig 2(b)). For the majority of the ELMy H-mode dataset, NTMs were absent. Almost all these discharges had sawteeth however. The transport coefficients discussed in this section are averaged over the occurrence of sawteeth and ELMs. The effects of these discrete MHD phenomena are discussed below. Over the ELMy H-mode dataset a strong inverse correlation of the anomalous tritium transport with plasma density

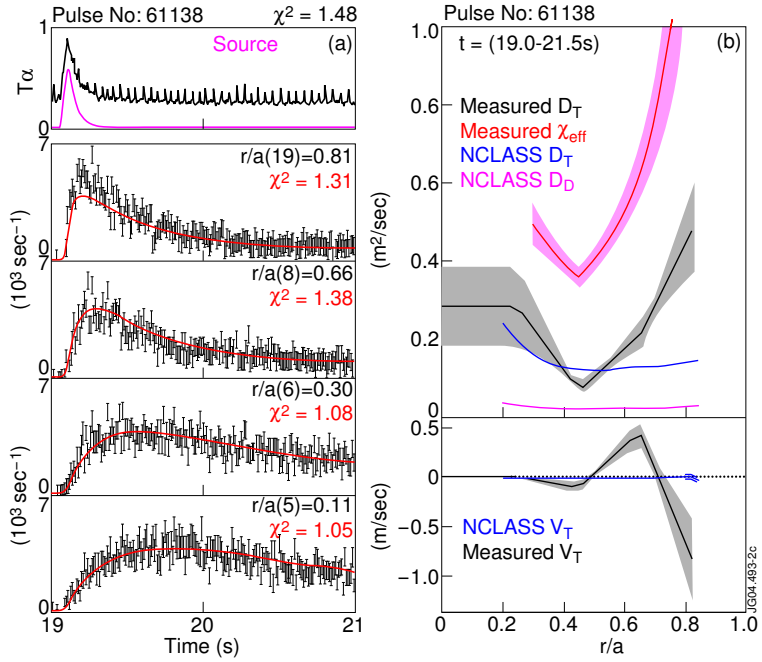

Fig.2 (a) Time evolution of the 14 MeV neutron signal in four individual chords of the neutron profile monitor, covering the range from the edge of the observed region to the core. The top frame shows the Tα input signal from the tritium gas puff. The fits to the data are shown (note all 19 camera channels are entered in the fit). (b) Tritium diffusion and convection coefficients for the fit to the high-density ELMy H-mode shot shown in (a), with comparison to the neoclassical predictions from NCLASS [11]. Shaded areas indicate the confidence limits for the fitted quantities.

was found: the D_T is close to its neoclassical value (as predicted using the NCLASS code [11]) at high density whilst the diffusion is strongly anomalous at low density. Likewise the tritium pinch (v_T) is closer to the neoclassical one in high density plasma, but it becomes highly anomalous at low density. As can be seen in Fig 2(b), the measured D_T remains above neo-classical in the outer part of the plasma (r/a > 0.6), but agrees with neo-classical predictions within r/a < 0.5. The thermal effective diffusivity does not display such strong density dependence leading to the density dependent ratio χ_{eff}/D_T.

Dedicated 'dimensionless variable' scans were also performed to study tritium transport in NBI-heated ,low q (q_{95} = 2.8), low triangularity (δ=0.2) ELMy H-modes of relevance to ITER. The details are given in a companion paper [12].

Scans were performed in each of ρ^* (Ion Larmor radius normalised to minor radius), ν^* (normalised collisionality ~ naq/T_e^2) and β (normalised plasma pressure), with the remaining two variables held approximately constant over the scan. The results showed that a strong 'Gyro-Bohm' like dependence on ρ^* in the inner part of the plasma ($D_T/B_0 \propto \rho^{*3.22\pm0.62}$, for 0<r/a<0.45) with a weaker 'Bohm' like dependence in the outer part of the plasma ($D_T/B_0 \propto \rho^{*1.9\pm0.38}$, for 0.65<r/a<0.80). For the ν^* and β dependence the following fits were obtained:

$$D_{T,inner} \propto \beta^{-0.34\pm0.08};\ D_{T,outer} \propto \beta^{-0.55\pm0.09};\ D_{T,inner} \propto \nu^{*-0.51\pm0.17};\ D_{T,outer} \propto \nu^{*-0.40\pm0.15}$$

The β and ν^* dependences for D_T are in strong contrast to the energy confinement scalings in the scans [12]: the energy confinement is largely independent of β, whilst the dependence on ν^* is actually in the opposite sense to particle confinement, with energy confinement decreasing weakly as ν^* increases. These results for ν^* are consistent with the density dependence seen generally in the χ_{eff}/D_T ratio.

In JET, plasmas with q_{min}~1, low positive shear, and no sawteeth have been developed in the so-called 'Hybrid' scenarios [13]. For these discharges the tritium transport following gas puffs and T^0 NBI was studied. The plasma triangularity was scanned (δ = 0.2 - 0.46), at constant energy confinement ($H\beta_N/q_{95}^2$ ~ 0.42). The raw decays of 14 MeV neutron signal following thermalisation of tritium fast ions from NBI, where wall sources were negligible, showed a global improvement in T particle confinement time (τ_{pT}^*) by ~ 50% over the scan. Fits were performed to the 14 MeV neutron signals following tritium gas puffs into identical discharges. The improvement in τ_{pT}^* was found to be explained in terms of a reduction in D_T across the whole plasma (although errors on the fits reduced the significance of this for r/a >0.5), whilst the values of v_T were independent of δ. In addition, I_p and B_T were varied at constant q_{95} and low δ. The neutron decay following T^0 NBI showed τ_{pT}^* scaled with I_p, and the detailed fits in the gas puff shots showed that the change was explained by a reduction in D_T confined to r/a > 0.5, although with less statistical significance than the triangularity scan. Again the fitted values of v_T were independent of I_p, B_T.

In ITB discharges with a strong single barrier [14], three features were observed: a reduction of D_T to neo-classical values in the transport barrier; an increase of D_T to large values in the region within the barrier; and a reduction of v_T in the barrier, see Fig. 3(c). The absolute value of v_T within the barrier remains above neo-classical values. The reduction of D_T in the barrier impedes tritium from reaching the core, whilst the increased D_T in the region enclosed by the barrier speeds up both the rate of rise to peak emission, and the decay rate after the peak emission seen by the innermost channels, in agreement with the line integrals measured by the cameras.

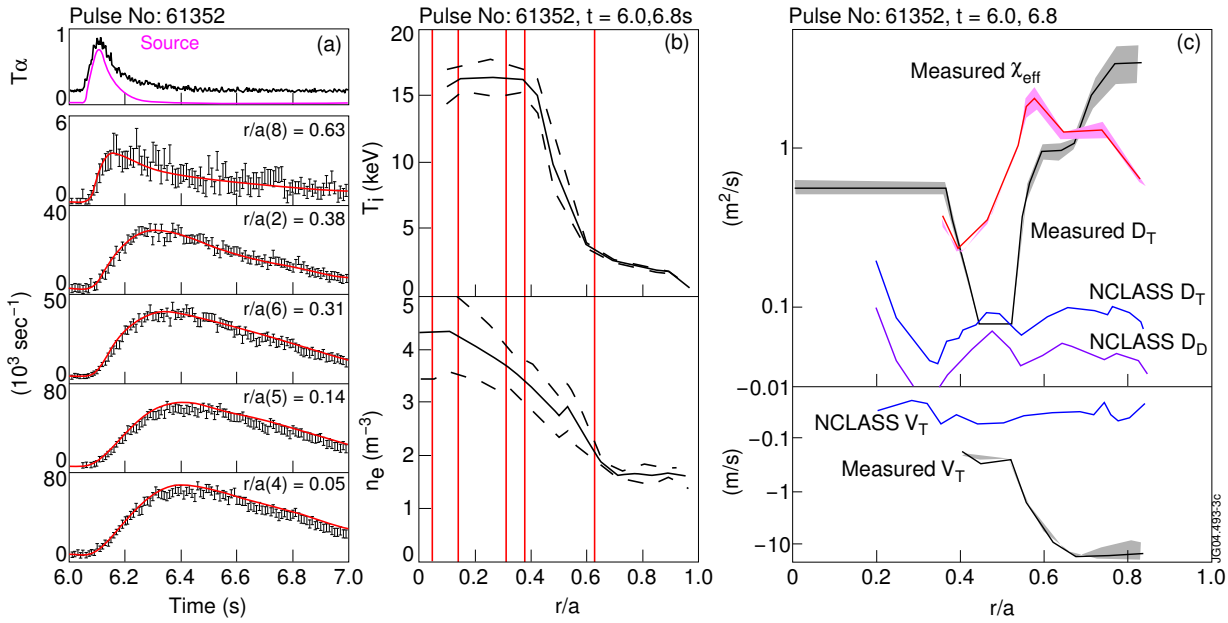

Fig.3 Tritium transport data and fits for a discharge with strong ITB and tritium gas puff. (a) Tritium gas source (via Tα measurement – top trace) and 14 MeV neutron signal time development for selected camera channels. (b) Ion temperature and electron density profiles for the ITB discharge with strong barrier present - vertical lines mark the radial positions of the camera channels in (a). (c) Fitted tritium diffusion coefficient and convection velocity spatial profiles for ITB discharge compared to neo-classical predictions from NCLASS code [11].

The data on ITB discharges have been interpreted to give preliminary results on the relative fuelling efficiency of tritium gas puffing, tritium recycled from the walls and T^0 NBI. Fig 4 (a) shows ion temperature (T_I) and electron density (n_e) profiles for three identical ITB discharges with a single strong barrier, the tritium fuelling being supplied by gas puff, T^0 NBI, and finally solely from wall recycling. The barrier measurements were made at suitable times (for the shot with T^0 NBI when the fast T^+ ions had thermalised, as calculated by the TRANSP code [15], for the gas puff shot when the tritium arrived in the core). The 14 MeV neutron emissivities for the three discharges are shown in Fig 4(b). The ratio of the total tritium atoms injected during a gas puff to that injected during the T^0 NBI pulse is ($3.1\ 10^{20}$ / $8.2\ 10^{18}$) ~ 38, whilst the ratio of the core emissivities in the two cases (~1.6), indicating that T^0 NBI is ~ 25 times more efficient at core fuelling. For discharges with weaker ITBs, although the T^0 NBI is always more efficient, the difference is not as pronounced, indicating that the relative fuelling efficiency depends on confinement inside the plasma. Details of tritium transport with ITBs present are given in [16].

The ratio of 25:1 advantage for T^0 NBI over T_2 gas puffing in the core of ITB discharges compares to an approximate 10:1 advantage for an ELMy H-mode plasma globally, inferred from the ~10% of tritium found inside the plasma at peak neutron emission following a tritium gas puff (see section 2). ELMy H-modes have been used to investigate the causes behind this global gas-fuelling efficiency. The neutron emission following the T^0 beam injection into a discharge is at first dominated by the non-thermal T^+ ions. Such discharges were analysed to give the rate of decay of the neutron signal after the fast ions had slowed down. This served as a constraint on the analysis of T_2 gas puff shots. The rate of decay in T_2 puff discharges, measured after the tritium ion density profile had fully relaxed, was always longer than the rate of decay after the T^0 beam injection. Of order 90% of the tritium after a gas puff is in or on the vessel wall and divertor tiles. Tritium released from these components acts as a fuel source and is responsible for the observed delay of tritium decay from the plasma. For the analysis of tritium ion transport a simple model for the flux in and out of the region observed by the neutron diagnostic was used with a quasi-realistic three-reservoir model (plasma, wall, divertor). Results using this model yielded physically plausible values for the free parameters: the fraction of tritium going direct to the wall

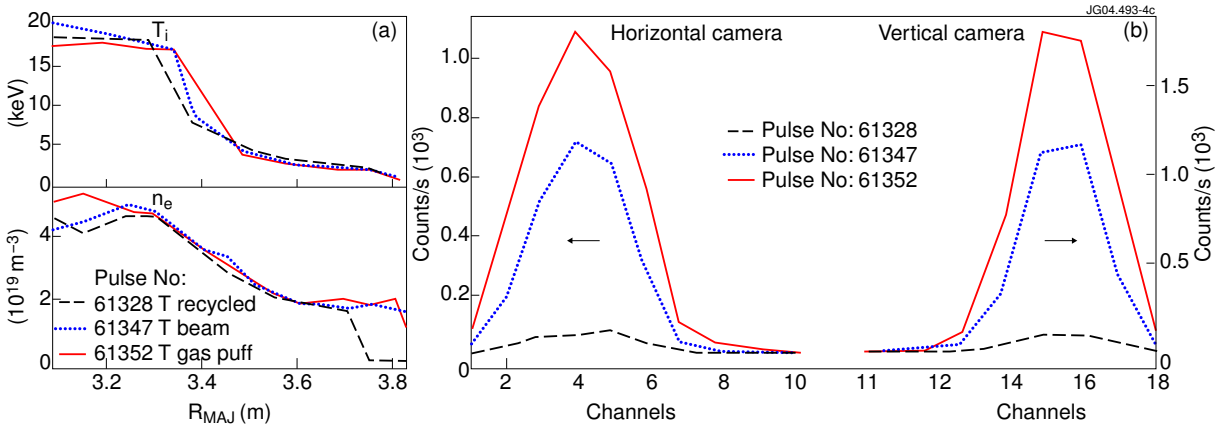

Fig.4 (a) Ion temperature and electron density profiles for three identical ITB discharges, two with tritium transient fuelling provided by T gas puff (shot 61352) and T^0 NBI(shot 61347) the third with tritium wall recycling only (61328). (b) 14 MeV neutron camera profiles compared for the three shots, at the time of the profiles in (a). At these times, for the transient shots, the T^0 NBI fast ions have slowed down (61347) or the T ions from gas puff have reached the plasma core (61352).

was ~ 0.6 (simple arguments of molecular breakup in the scrape-off layer would give ~ 0.5), and typical wall retention times ~ 0.2 -0.5 s. were found (of the order of the plasma energy confinement time). The divertor retention time was longer than 5 s. The gas fuelling efficiency data thus yields a picture in which: around 60% of the gas goes direct to the wall, and is then desorbed easily by the plasma heat efflux on an energy confinement scale; and ~ 30% is transported quickly out of the outer region (r/a > 0.85), and deposited in the divertor, with a much longer characteristic timescale for return. Of the ~ 10% entering the plasma, there is a further barrier to fuelling the core presented by an ITB. Such fuelling considerations will be important in the transient phase of ITB scenarios used to start up burning D-T plasmas.

For a comparison of the scaling of transport in the different regimes studied, the analysis has focussed on the outer region observed by the neutron cameras, i.e. 0.65<r/a<0.80. In the central region, differences between ELMy H-Mode discharges (q_0<1, exhibiting sawtooth behaviour), hybrid scenarios ($q_0 \approx 1$) and ITB discharges (q_0>2 or even q_0>3) can be expected. In contrast, tritium transport well outside the central region should be comparable between all scenarios.

There was a strong correlation for all three scenarios of D_T with q_{95} (scanned by varying current and toroidal field) for 0.65<r/a<0.80. Energy transport in the same discharges, characterized by χ_{eff}, was not strongly affected, and thus D_T/χ_{eff} varied between 0.3 (high density, low q_{95}) and 2.0 (low density, high q_{95}). Initial results show plasmas with added ICRH have a larger ratio of D_T/χ_{eff}, a phenomenon still under investigation. D_T correlates better with the local value of q, suggesting that the orbit width of trapped particles is an important parameter determining the scaling. Fig. 5 shows the relationship of the normalized diffusion coefficient D_T/B_ϕ [17] with the

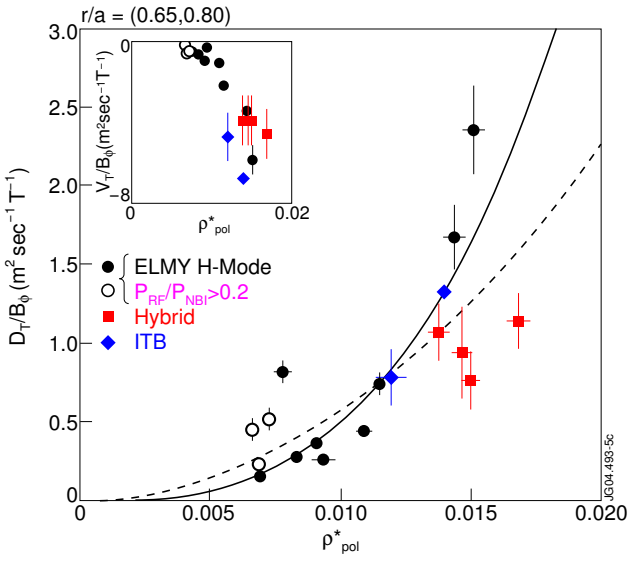

Fig.5 Plot of normalised D_T/B_ϕ and v_T/B_ϕ against local poloidal Larmor radius ($\rho^*_{pol}=q\times\rho^*$) for 0.65<r/a<0.8 in various JET discharge regimes. The solid line corresponds to Gyro-Bohm scaling ($\rho^*_{pol}{}^3$), the dashed line to Bohm scaling ($\rho^*_{pol}{}^2$).

normalized poloidal Larmor radius $\rho^*_{pol}=q\times\rho^*$ (where $\rho^* \sim T_i^{1/2}/aB$). This results in a very strong correlation for the ELMy H-Mode discharges alone, which is better described by gyro-Bohm scaling ($\rho^*_{pol}{}^3$) rather than Bohm scaling ($\rho^*_{pol}{}^2$). Note how the inclusion of q in the scaling parameter has now altered the conclusion with respect to Gyro-Bohm/Bohm scaling reached in the dimensionless parameter scans [12]. With ρ^*_{pol} as scaling parameter differences appear for hybrid scenario discharges and for discharges with significant ICRH heating, whilst the two ITB discharges agree with the trend within errors. Fig. 5 also shows an equally strong trend for v_T/B_ϕ with local ρ^*_{pol}. In this inset, the hybrid scenario discharges follow the trend of the ELMy H-Mode discharges, whereas the ITB discharges stand out. The ratio of v_T/D_T, which determines the profile shape, varies from –2 m^{-1} for high q, low density to ±0.1 m^{-1} at low q, high density.

The hybrid scenario discharges are characterised by larger β, and the behaviour of D_T with β is consistent with the fits to ELMy H-mode data in the specific dimensionless parameter scans (described above). Similar inverse β–dependence was found on DIII-D for helium particle transport [18].

Sawtooth collapses resulted in tritium density-profile changes [19]. The dominant contribution to the observed changes of the neutron line integrals is the redistribution of fast NBI-derived deuterium ions. At the time when they disappeared from the central channels (evident from a dip in the central line integrals), a burst of 14 MeV neutrons was seen in channels with an impact parameter as far as r/a≈0.5. Sawtooth collapses that occurred during inward propagation of tritium, i.e. shortly after the puff, did not exhibit this feature: the ejection of deuterium ions from the core being compensated by the tritium ions being swept into the core, keeping the line integrals almost constant. Sawtooth effects were most pronounced at low density, where the NBI deuterium ion density was more peaked.

ELMs that occured during the time of the puff resulted in a noticeable increase of 14 MeV line integrals with an impact parameter as far into the plasma as r/a≈0.5 within 10 ms. We do not have a quantitative understanding of this effect, but changes in ELM frequency should result in changes to the fuelling efficiency of tritium on the assumption that D_T during an ELM rises significantly above the level of D_T between ELMs [20]. The transient effects could be the result of deeper fuelling due to charge-exchange as a result of the increase of the deuterium neutral flux after the ELM, but note that simultaneously losses due to charge-exchange would also increase, leading to a null effect. It is also possible that tritium neutral influx increases as a result of energy or particles released from the plasma during the ELM, dislodging tritium from the wall or divertor. The combination of all three effects will require further analysis to elucidate.

The effect of NTMs was studied in pairs of discharges with near identical plasma conditions, one with and one without a 3/2 NTM [21]. Changes to 14 MeV line integrals were observed for lines-of-sight with an impact parameter inside the region of q<3/2. Allowing for the slight differences in temperature and density between the discharges, the major part of the changes require a change in the tritium transport, localized at, or within, the q=3/2 surface. Both changes in D_T and v_T are consistent with the observations, but the effect of the NTM on fast ions (which mainly determine the neutron emission in this region) requires further modelling to reach a firm conclusion.

4. Fast particle transport

Tritium NBI ions were used in several fast particle transport experiments. The confinement of tritium beam-ions was studied in reversed-shear (ITB) and 'current-hole' plasmas. The effect of Toroidal Alfven Eigenmode (TAE) and Fishbone modes on fast T ion transport was also studied. For diagnosis of the alpha particles (α) produced in the D-T reactions the diagnostic method based on γ-rays from the $^{9}Be(\alpha,n\gamma)^{12}C$ nuclear reaction was used. During TTE the slowing down of fusion born alphas was measured for the first time with this approach, using a well shielded high-efficiency γ ray spectrometer based on a bismuth germanate (*BGO*) detector [22].

In JET plasmas with a Current Hole (CH) the toroidal current density falls to near zero for typically 1/3 –1/2 of the minor radius [23], and there is an ITB near the edge of the CH. These

plasmas are expected to confine fast ions poorly as a result of the very low central poloidal field (B_θ). The effect of a CH on fast beam ions was demonstrated by measuring the 14 MeV neutron profiles from the interactions of 105 kV triton beam ions with the background deuterium. As the D-T reactivity (σv_{DT}) decreases rapidly with triton energy, the information covers the fast triton behaviour in a narrow energy range E_b-E<<E_b, (where E_b= 105 kV). Tritons were injected into both CH and Monotonic Current profile (MC) plasmas with the same plasma current (1.5 – 2 MA), and the triton beams were injected both on and off the magnetic axis (in the vertical dimension). For on-axis injection, the measured neutron profiles demonstrate an outward shift induced by the CH (Fig 6(a)) whilst for off-axis tritons (not shown) the peak is shifted inwards.

The behaviour of the fast beam tritons has been modelled with a 3-D Fokker-Planck code [24], and also in TRANSP [25]. For individual tritons, consideration of the orbits shows that the maximum ion density corresponds to a midplane radius where beam tritons execute near-'stagnation' orbits, with radial and vertical drift velocities near zero. For on-axis beams, stagnation orbits are normally realised close to the magnetic axis (low B_θ), however, the large radial extent of the low B_θ region in a CH plasma causes an outward shift in the stagnation point. The results of the 3-D Fokker Planck model show a satisfactory explanation for the measured 14 MeV profiles. As an example, Fig 6(b) shows the modelled profiles for on-axis triton beam injection into a CH plasma, which compare qualitatively with the data. The TRANSP modelling also shows qualitative agreement (Fig 6(c)). The centroid of the neutron distribution was measured by averaging the yields in the camera inner channels. This centroid was seen to move as the edge of the CH region, as established by the Motional Stark Effect (MSE) diagnostic [25], moved with the current profile evolution. Occasionally, the CH was instantaneously eroded by MHD activity, and in these cases a corresponding step change in the neutron profile centroid was seen (Fig.7).

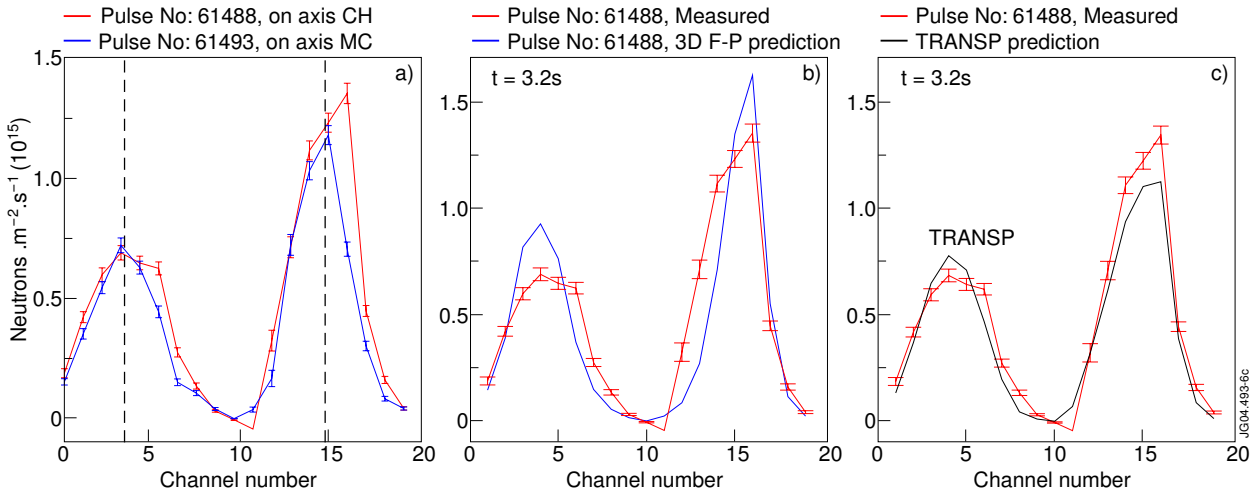

Fig.6 (a)Neutron emission profiles from the vertical and horizontal cameras for on-axis T^0 NB injection in the case of current hole(CH) and monotonic current (MC) profile plasmas. Vertical dashed lines indicate the axis of the plasma for the two views. (b) Comparison of Fokker Planck (F-P) code prediction for neutron profiles and neutron camera data for the case of on-axis injection into the CH discharge. (c) Comparison of TRANSP code prediction for neutron profiles and neutron camera data for the same on-axis injection case as in (b). Measurements and predictions correspond to the end of 200 ms NBI pulses

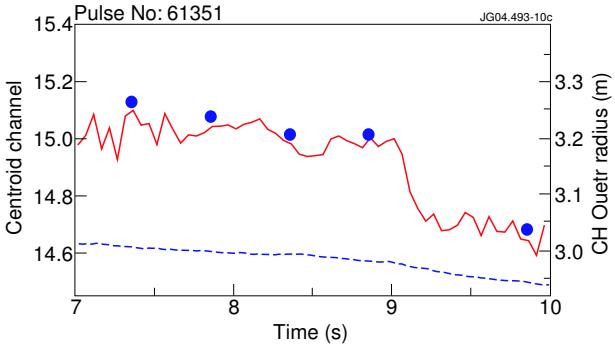

Fig. 7 Centroid movement for 14 MeV neutron emission profile (solid line) compared to shrinkage of the current hole (circles). Dashed line shows the magnetic axis position.

The decay rates of γ-rays from reaction $^{9}Be(\alpha,n\gamma)^{12}C$ following T^0 NBI pulses were measured in many TTE discharges. This decay rate can be related to the combined slowing down of the parent beam tritons ($\tau_{SD,T}$) and the alphas ($\tau_{SD,\alpha}$) subsequently produced [22]. The combined value of ($\tau_{SD,T}+\tau_{SD,\alpha}$) can be compared to the measured γ decay, as in Fig 8. In discharges with relatively high monotonic currents (I_p>2MA) the observed density decay of fast ions inferred from γ-ray measurements was consistent with classical slowing down, while in 2.5MA discharges with a current hole as large as about 1/3 of the plasma radius the measured decay time was much shorter than the classical slowing down time, indicating confinement degradation of fast alphas similar to that seen at low current (I_p=1MA). The confinement of charged fusion products (CFPs) has been modelled with the 3D Fokker-Planck (F-P) code in reversed shear plasmas in the axi-symmetric limit [24]. The 3-D code takes into account the combined effects of alpha loss and transport out of the detector line-of-sight. A strong effect of reversed shear on CFP confinement is found when the plasma current is less than the critical current, I_{cr}, required to confine the fattest bananas crossing the plasma core [26]. I_{cr} increases with the size of the "zero" poloidal field region, r_*/a, and for typical JET CH discharges exceeds 4 MA for 3.5 MeV alphas if r_*/a > 0.4. In MC plasmas, this critical current, I_{cr0}, is of order 2 MA. The confinement of CFPs in CH discharges (strong RS) with r_*/a > 0.4 is significantly degraded compared to MC plasmas even at relatively

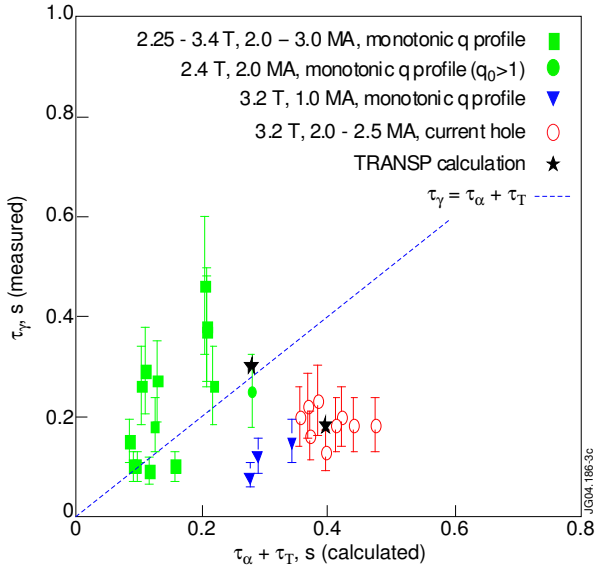

Fig.8. Measured 4.44-MeV gamma-ray decay-times due to the Be+alpha nuclear reaction vs. calculated classical slowing down-times of T-beam ions and alpha particles for plasma scenarios with: B_T=2.25-3.2T, I_p=1.0-3.0MA.

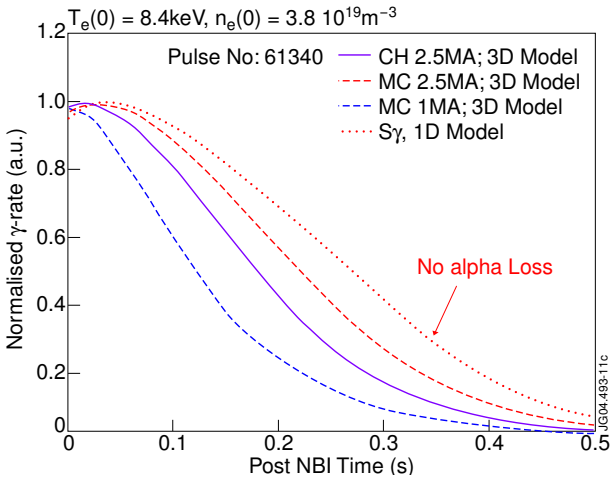

Fig.9 Normalised γ-decay rate (post T-NBI) from 3-D Fokker Planck (F-P) code simulation for I_p=2.5MA Current Hole (CH) pulse 61340, with central parameters as shown and CH radius r_*/a ~0.57(solid curve). Dashed curves are 3-D F-P results for Monotonic Current (MC) plasmas with same T_e, n_e profiles and I_p as shown. Dotted curve shows 1-D F-P model for I_p=2.5MA MC plasma.

high plasma currents I_p=2-2.5MA. For low currents, where $I_p<I_{cr}$, strong RS results in a substantial reduction of the density of fast CFPs due to confinement degradation and spatial redistribution both effected by the ion orbit topology modification. Calculated decay rates of fusion alphas along the JET γ-ray spectrometer observation line of sight are displayed in Fig. 9. The case with large CH at I_p = 2.5 MA correponds to a TTE discharge pulse 61340 with measured $T_e(0)$ = 8.4 keV and $n_e(0)$ = 3.8 10^{19} m^{-3}. Other curves compare postulated plasmas with the same T_e and n_e profiles but MC profiles. The reduction in γ -rate, and in γ-decay time for the CH case are clearly seen. Thus, in agreement with experiment, and TRANSP simulations (Fig.8), the 3D F-P code shows that RS decreases the decay time of the fast alpha distribution.

The evolution of T^+ fast ions from T^0 NBI with velocities comparable to the Alfven velocity was investigated in TTE discharges with B_T=0.86 T, I_p=0.9 MA. The deuterium (D^0) NBI was used at power levels > 5 MW to destabilise TAE and n=1 Fishbones. The 14 MeV neutron camera profiles' evolution was measured during four 50 ms pulses of T^0 NBI injected on top of the D^0 heating. The effects of fishbones were seen, as loss of central fast ions, on the T^0 NBI deposition profiles: although these effects were not as large as those observed in earlier JET 10:90 D-T plasma experiments [27], at higher powers and similar plasma current and q. No appreciable effect was found for low amplitude TAEs. Details of the experiment are given in ref [28].

5. Summary

Thermal tritium particle transport coefficients (D_T, v_T) were found to substantially exceed neo-classsical values in all regimes except in ELMy H-modes at high density , and in the region of ITBs in RS plasmas. In hybrid scenarios, increasing triangularity and plasma current raises particle confinement time, but transport remains in excess of neo-classical values. Comparing different regimes (ELMy H-mode, ITB plasma, and Hybrid scenarios) outside the central plasma region (0.65<r/a<0.80), the tritium diffusion coefficient (D_T/B_ϕ) scales in a manner closer to Gyro-Bohm ($\sim\rho_\theta^{*3}$, where $\rho_\theta^*=q\rho^*$), but with an added inverse β dependence. In contrast, for ELMy H-mode discharge pairs with all dimensionless parameters except ρ^* kept constant, Gyro-Bohm behaviour is confined to the inner part of the plasma (r/a<0.4), and the outer plasma behaves more like Bohm ($\sim\rho^{*2}$). Similar dimensionless parameter scans established contrasting trends for particle confinement (increases with ν^* and β) and energy confinement (decreases with ν^* and independent of β). 3/2 NTMs affect tritium transport within the q=3/2 radius.

The effects of a Current Hole in the centre of JET plasmas on fast injected NBI ions can be seen as outward shifts in the deposition profile for on-axis injection. This is qualitatively explained by a 3-D Fokker Planck numerical code and TRANSP modelling. γ-ray emission decay times from nuclear reactions between fusion alphas and beryllium impurities ($^9Be(\alpha,n\gamma)^{12}C$) are consistent with classical alpha (and parent triton) slowing down times for high plasma currents (I_p >2MA) and monotonic q-profiles. γ-ray emission decay times are much shorter in CH plasmas, indicating alpha confinement degradation, due to orbit losses predicted by the 3-D Fokker Planck code.

Acknowledgement

This work was performed under the European Fusion Development Agreement, and funded partly by the UK Engineering and Physical Sciences Research Council and by EURATOM.

References

[1] KEILHACKER, M., Phil.Trans.R.Soc.London A **357** (1999) 415.
[2] MATTHEWS, G.F., et al., J. Nucl. Mater. **266-269** (1999) 153
[3] THE JET TEAM, presented by ZASTROW, K-D., Nucl. Fusion **39** (1999) 1891
[4] EFTHIMION, P., et al., Phys. Rev. Letters **55** (1995) 85
[5] EFTHIMION, P., et al., Nucl. Fusion **39** (1999)
[6] MURARI, A., et al., "New developments in JET Neutron, Alpha Particle and Fuel mixture diagnostics with potential relevance for ITER", these proceedings, Paper OV/P4-9.
[7] JONES, T.T.C., et al., "Technical and scientific aspects of the JET Trace-Tritium experimental campaign"", 7th Conference on Tritium Science and Technology, Baden-Baden, Germany, 2004. To be published in Fusion Science and Technology.
[8] BERTALOT, L., et al., "ITER relevant developments in neutron diagnostics during the JET Trace Tritium Campaign", Proc. 23rd Symposium on Fusion Technology, Venice, 2004.
[9] POPOVICHEV, S., et al., "Performance of Neutron Measurements during Trace Tritium Experiments on JET", Proc. 31st EPS Conference on Plasma Physics, London 2004, P5-173
[10] ZASTROW, K-D., et al., "Tritium Transport Experiments on the JET Tokamak", 31st EPS, London 2004, accepted for publication in Plasma Phys. and Controlled Fusion.
[11] HOULBERG, W., et al., Nucl. Fusion **34** (1994) 93
[12] MCDONALD, D.C., et al., " Particle and Energy transport in dedicated rho*, beta, and nu* scans in JET ELMy H-modes", these proceedings, Paper EX/6-6.
[13] JOFFRIN, E., et al., "The hybrid scenario in JET: towards its validation for ITER", these proceedings, Paper EX/4-2.
[14] TUCCILLO, A.A., et al., "Development on JET of Advanced Tokamak operations for ITER", these proceedings, Paper EX/1-1
[15] GOLDSTON, R., et al., J. Comput. Phys. **43** (1994) 93
[16] MAILLOUX, J., et al., "Tritium Fuelling of JET plasmas with Internal Transport Barriers", Proc. 31st EPS Conference on Plasma Physics, London 2004, P1-148
[17] CONNOR, J .W., and TAYLOR, J. B., Nucl. Fusion **17** (1977) 1047
[18] PETTY, C. C., et al., Phys. Plasmas **11** (2004) 2514
[19] VOITSEKHOVITCH, I., et al., "Transport analysis of trace Tritium experiments on JET and comparison with theory-based transport models", Proc. 31st EPS Conference on Plasma Physics, London 2004, P1-158
[20] BELO, P., et al., "Role of impurity and deuterium fuelling in evolution of trace tritium in JET ELMy H-mode: transport analysis and predictive modelling", ibid., P1-169
[21] HENDER, T .C., et al., "Trace-Tritium Measurement of Magnetic Island Effect on Particle Confinement", Proc. 31st EPS Conference on Plasma Physics, London 2004, P1-163
[22] KIPTILY, V., et al., Phys.Rev.Letters **93**(11) (2004) 115001
[23] HAWKES, N.C., et al., Phys.Rev.Letters **87** (2001) 115001
[24] YAVORSKIJ, V., et al., "Confinement of charged fusion products in Reversed Shear tokamak plasmas", these proceedings, Paper TH/P4-49.
[25] HAWKES, N.C., et al., "Tritium fast ion distribution in JET current hole plasmas", in preparation for Plasma Phys and Controlled Fusion.
[26] YAVORSKIJ, V., et al., Nucl. Fusion **44** (2004) L5-L9.
[27] BORBA, D.N. et al., Nucl. Fusion **40** (2000) 775
[28] SHARAPOV, S.E., et al., "Experiment on tritium beam evolution in JET plasmas with Fishbones and TAE mode.", Proc. 31st EPS Conference on Plasma Physics, London 2004, P5-166